

# Imaging Underwater Objects with Ambient Noise

Aron C. Atkins

Henry A. Fink

Jeffrey D. Spaleta

{ atkins, haf, spaletaj } @wpi.edu

Worcester Polytechnic Institute

Worcester, MA 01609

Advisor: Arthur C. Heinricher

## Introduction

We present a method of locating and tracking undersea objects of various sizes. We list assumptions that help define our approach, together with requirements that must be met for an object to be detectable. We construct a detection scheme for two dimensions, which we generalize to three dimensions.

In constructing our models, we make several design decisions which include time limitations, range, and space and resource requirements. Many of these choices are desirable for confidently detecting objects.

## Assumptions

We make several assumptions regarding the type of environment to which we will be listening.

- We consider an extreme case in which our object must be a near-perfect acoustic reflector; such an object resembles a submarine, which tends to absorb very little sound. (If submarines absorbed a predominant amount of sound, sonar systems would be ineffective in tracking their movement.)

By requiring our target object to be a near-perfect acoustic reflector, an individual scanning frequency can be chosen from a range of transmittable frequencies in ocean water. This range is given as between 5 and 50 kHz [Buckingham et al. 1992]. We can limit our monitoring process to a single frequency because a near-perfect acoustic reflector will give the same characteristic response at all frequencies [Pedrotti and Pedrotti 1993]. Having information on more than one frequency would produce redundant information. It is better to pick a single frequency that is strongly represented in the ambient noise field than to monitor several different frequencies.

- We require directionality in the ambient field. Without an ambient noise bias in some direction, there will not be a detectable difference between reflected and background noise. Experimental research shows there is a directional bias in the ambient noise field near the ocean's surface and floor [Stephens 1970, 124–125; Urick 1983, 227]. For acoustic absorbers, ambient field directionality would be unnecessary; absorbers would always be detected as “holes” in the ambient noise field intensity regardless of field bias.
- We also require that the ambient noise field remain relatively stable while we are searching. Frequent changes in the field over short time intervals make it nearly impossible to find an object.
- We require that at least one of the following two conditions holds to detect confidently the presence of objects in our scan region:
  - The object being scanned is in motion relative to our scan location.
  - We perform a background scan prior to the target object entering into our scan region, reliable for the ocean conditions during the search time.
- We assume a minimum target size of approximate 10 m, the average width of submarines in the U.S. Navy. Submarines of other nations are of comparable size.
- Our sensing equipment consists of multiple parabolic reflectors, commonly used for focusing weak signals to one focal point, where we place a hydrophone, a device designed to measure acoustic intensity under water [Geil 1992]. This type of sensor has been used previously in related experiments [Buckingham et al. 1992] with promising results. Additionally, we assume that our equipment can detect angle differences to  $0.1^\circ$ .

We would like a system capable of detecting objects as far away as possible for relatively small sensor size. The relation between resolving distance and sensor diameter is given in **Appendix A**.

## Object Detection

### Prior Experimental Results

Our procedure relies on the results of an experiment performed by Buckingham et al. [1992] in which neoprene-coated boards submerged near a pier were detected using the ambient noise in the water. In their experiment, three targets each 0.9 m high and 0.77 m wide were placed 7 m from a reflector. The detector was a hydrophone located at the focal point of a parabolic reflector of diameter 1.22 m with a neoprene rubber surface. The back of the hydrophone was shielded to prevent detecting noise from that side. The boards first were

turned edge-on to the reflector and the noise level was recorded over a frequency range of 5–50 kHz. When the boards were rotated so that they were face-on to the parabolic dish, the noise spectrum was recorded again. By subtracting the two spectra, the authors found an average intensity difference of 4 dB. They reasoned that this difference was due to a directionality in the noise emanating from the nearby pier.

Our procedure for detecting objects in the ocean using the ambient noise field extends this experiment. We first consider locating and tracking an object in the ocean in two dimensions, using two of these reflectors.

## Object Detection in Two Dimensions

We can uniquely determine any point in the plane if we know its distance from two known points. These known points can be our parabolic reflectors. (We assume that the object moving through the ocean is never collinear with our two reflectors; if there is reason to believe this may happen, we can add a noncollinear third reflector.)

To simplify visualizing the problem, we consider the special case when both of the parabolic reflectors are located at a fixed depth near the shore line; this does not make the problem any less interesting and is likely to be the case in many practical implementations (see **Figure 1**). The process of detecting a distant object begins with both reflectors sweeping through  $180^\circ$  while monitoring a fixed frequency. If the background noise were constant for all angles, then a plot of noise vs. angle would yield a horizontal line. However, due to directional biases in the ambient noise field, it is likely that this noise will be a function of the angle at which the reflector is directed. For this reason, it would be useful to have a background scan (a scan with no object present) for comparison with later scans.

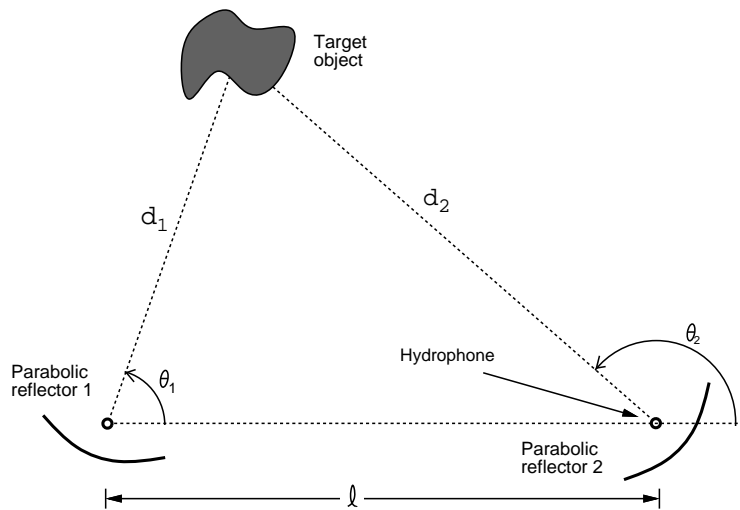


**Figure 1.** Point location in two dimensions.

Assuming that a background scan has been made, it is a simple matter for both reflectors to scan through angles and record the ambient noise level when searching for an object. By subtracting away the two plots of noise level in dB vs. the angle each reflector has swept from its initial position, a characteristic disturbance pattern should appear over a small angle range, indicating the presence of an object. The angle at the center of this disturbance represents the approximate viewing angle to the center of the object. Knowing this angle measurement from each reflector and the distance between the reflectors, it is a simple matter to triangulate the position of the object. A method to perform this triangulation is described in **Appendix C**.

The disturbance pattern in the intensity plot gives more information than just the viewing angle at which the center of the object is located. Since the angle is being swept out, the broader the disturbance pattern, the larger the object. By measuring the angular width of the disturbance region, we can calculate an approximate size of the object. Once the distance to the object has been found, the triangulation formulas can be applied using the extreme angular values of the signal disturbance to find the size of the object. The size of the object is approximated from the difference between the two extreme locations calculated from triangulation.

Once the reflectors have found the object initially, they can track it by scanning through a small interval centered around the initial position. This interval can come from an estimate of the velocity of the object.

One possibility that can occur while scanning is that the object could be out of range of one of the two reflectors. The position of the object can still be approximated, since the ranges of both of the reflectors are known. The object would lie in crescent region inside the circle of detection of one reflector and outside the circle of detection of the second. This gives a rough location of the object that may be good enough in practical applications. A potential intersection of two sensor regions is shown in **Figure 2**.

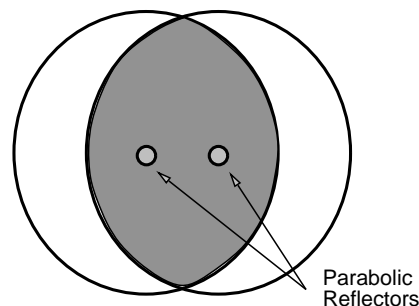


**Figure 2.** Intersection of two scan regions.

## Detection without a Background Scan

If a background scan is not available, or if the background noise has changed sufficiently (due to a storm or other disturbances in the ocean), then an object

can still be detected and tracked. Again, for simplicity, we consider the case where the reflectors lie along a shore. The process begins as before, with each reflector sweeping through  $180^\circ$  and recording the ambient noise level. This scan will be a combination of the background noise with the influence of an object, if present. Although a variance may be present in this scan, it cannot be ruled out that its presence is merely an artifact of the normal ambient noise at that angle. To determine whether there is a true disturbance, a second full scan is needed a short time later.

Once a second scan has been made, the two can be subtracted as before to yield the difference in noise level at each angle. Assuming that the target object has moved during the two scan periods, there will be a shift in the disturbance on the second noise plot. The subtraction will yield a pattern. The midpoint in the subtracted disturbance region gives an approximation to the angle at which the object was viewed halfway during the time interval. If the two scans are taken close enough together to narrow down the time, yet far enough apart to detect the shift in the object's position, then the position of the object can be determined with nearly the same accuracy as when a background scan is used.

The drawback to this approach is that it requires each reflector, at least initially, to scan through a full  $180^\circ$  ( $360^\circ$  when not near the shore) at least twice to detect the object. Once the object is found, two passes over a much smaller angular range can be used to track it as before. A second shortcoming is that the method can detect only moving objects. To detect a stationary object, a background scan is required.

## Object Detection in Three Dimensions

Three-dimensional object detection requires substantially more time than the two-dimensional case (see **Figure 3**). Each reflector has to sweep out the entire volume of space, a formidable task. The position of an object can be determined from the angles to it from two known points, just as in the two-dimensional case. The direction of each reflector is described by two angles, using their spherical coordinate representation, or alternatively by vectors. The case of both reflectors and the object being collinear can be resolved by using a third noncollinear reflector.

## Ideal Detection of Objects

To cover a large region effectively, we use an array of reflectors positioned so that each point lies within the range of at least two reflectors. An ideal object-location scheme would use not two but three (noncollinear) parabolic reflectors to detect objects in the scan region. An object entering the region would be detected immediately by at least one reflector. Then the remaining reflectors would scan along the line of sight of the first reflector until they detect the object. Next, the three-dimensional point-location scheme discussed

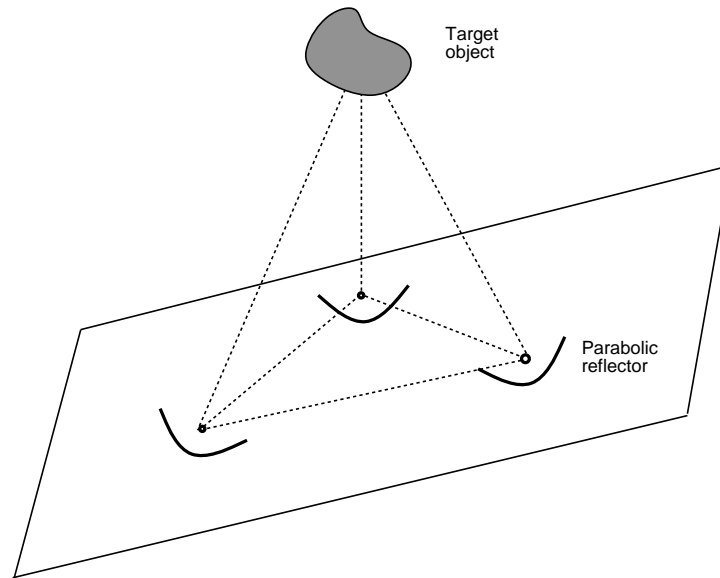


**Figure 3.** Point location in three dimensions.

in **Appendix D** determines the object's position. With a second scan a short time later, the two positions determine the heading and velocity.

## Detection with Reflector Arrays

A major problem with our scheme is that it does not produce a complete sweep of the full area in a reasonable time. We can compensate for this by adding additional reflectors or by changing the shape of the reflectors. The array configurations we consider are a trough system (**Figure 4**), a linear system (**Figure 5**), and a parabolic torus configuration (**Figure 6**).

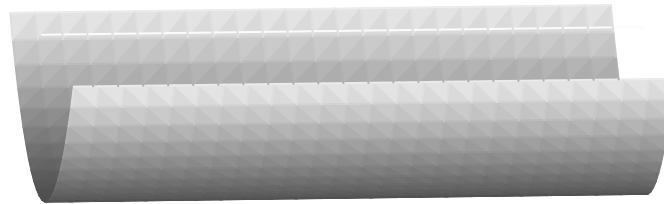


**Figure 4.** Parabolic trough.

### The Parabolic Trough

Parabolic troughs were used as solar energy collectors as early as the late 1800s, to focus the sun's energy to heat water-filled pipes. Many solar energy plants still use parabolic troughs because of their advantages over flat mirrors or dishes [Smith 1996].

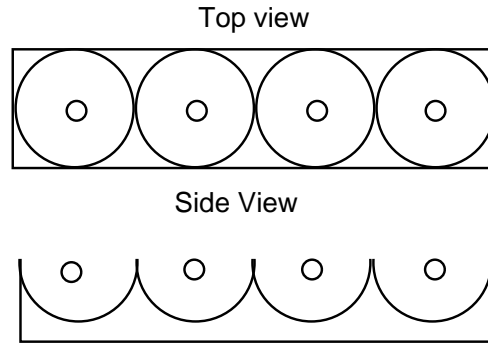


**Figure 5.** Linear array configuration.

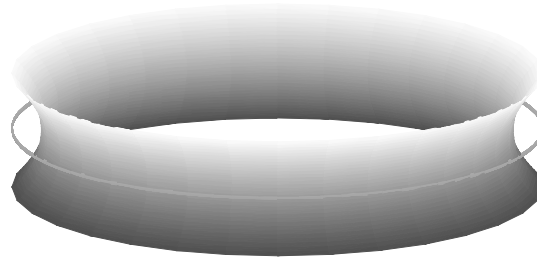


**Figure 6.** Parabolic torus.

A parabolic trough is shaped something like a soup can cut in half length-wise. Unlike a parabolic dish, which only focuses rays to a specific focal point, a parabolic trough focuses rays into a line. A parabolic trough is simpler and cheaper to construct than a parabolic dish and can scan a much wider field. An array might be constructed of three of these parabolic troughs oriented at different angles. As each of them rotates, they sweep out a plane. The intersection of these three planes gives the location of the object. It is unlikely that an object would evade detection if the troughs are long enough and are able to rotate through some angle to compensate for their finite length.

A drawback to using a parabolic trough is its inefficiency, since it focuses rays to a line rather than a point. This would lead to lower detected intensities when an object is encountered.

## The Linear Array

The same effect of using a trough can be produced using a linear string of dishes. If all the reflectors point in the same direction, then this would act as a trough with a finite number of focus points. The disadvantage is the cost of construction and the need for careful alignment of each dish.

## The Parabolic Torus

A parabolic trough still does not sweep out an infinite plane through its rotations. One reflector shape that can focus the ambient noise in an entire

plane into a detectable area is a parabolic torus, which looks like a tire rim. Each cross section is a parabola, so the parabolic torus focuses energy a constant distance away from the vertex. For this torus, the focus becomes a ring around the reflecting surface. In theory, this provides a tremendous advantage over either troughs or dishes. A trough is limited to scanning areas only as wide as its length. The parabolic torus scans an entire plane during one instant and, when it is swept through  $180^\circ$  perpendicular to its axis, scans the entire volume around it. Thus, it is impossible to “hide” from this sensor, as is possible with the previous two.

A weakness of this reflector construction is that even less energy is focused from an object in the surroundings than from a parabolic trough. Unless the object creates a strong disturbance pattern in the ambient noise field, the object may not be seen with this reflector. Additionally, we can expect the range of this system to be less than for a system using only parabolic dishes.

A detection system could then employ three of these reflectors mounted at different angles. Each would sweep through their surroundings. After a full revolution, they would have two scans and corresponding angles for each scan.

A more accurate procedure might use two parabolic tori and a parabolic dish. The tori could be used to find the line along which the object lies and the dish could then sweep out along that line with greater accuracy to find the object. A drawback of the tori configuration is that we do not know a way of calculating the resolving power, so we do not know the range.

## Strengths and Limitations

We discuss the necessity of some of our assumptions and what happens if they are relaxed or removed. We also reveal some intrinsic limitations due to equipment and environment.

- We can relax our assumption that the target object is a near-perfect reflector. Strong sound-absorbing objects produce intensity profiles with negative difference regions compared to the background, in contrast to the positive regions for near-perfect reflectors. The similarities suggest that our assumption is not needed. If we allow frequency-dependent reflectivity, we can determine the acoustic color of an object by scanning over a range of frequencies.
- If the assumption requiring directionality is removed, detection becomes difficult for all objects except very strong acoustic absorbers. Absorbers would always show up as “holes” in the background ambient noise field. Since interesting strong acoustic absorbers are rare, we recommend that this constraint remain in any implementation.
- There is no need for a background reference scan if we use a multiple scanning technique on moving objects. If a reliable background scan can be



obtained, it should be used for validation; for detection of stationary objects, a confident background is still necessary.

- Ambient noise near the surface of the ocean is unstable because of highly variant surface conditions, so stationary objects would be harder to detect. This is contrasted by the seismically directed field at the ocean floor, which is constant over periods as long as seasons [Stephens 1970].
- We are uncertain which reflector type is the best in practical situations. We suggest experimentation like that in Buckingham et al. [1992].
- The angle-measuring precision of our tracking equipment is crucial to our ability to precisely find objects. If we alter the precision of our equipment even slightly, we might incorrectly locate the object, especially when it is far away.
- We must limit the total size of our reflector. Large reflectors are impractical because moving them underwater poses a significant problem and because one placed on a ship must not restrict the ship's movement.
- One last limitation that dominates any design is the acoustic energy absorption of sea water. This attenuation of energy effectively cuts our viewing distance to 1 km if we are using a frequency of 40 kHz [Stephens 1970, 12], which is disappointing.

## Conclusions

Our findings lead us to believe that this technology is a viable detection system for most circumstances. Theoretical results for distant objects, or for stationary objects in unstable ambient fields, are not so positive; and this type of system would be not advisable for these conditions. We are disappointed in the limited maximum viewing range in ocean water. The range of 1 km greatly limits the ability to detect approaching submarines.

This is, however, a great way to detect stationary submarines at deeper levels, which are hard to detect using traditional sonar techniques [Stephens 1970]. A scan depth of 1 km is a reasonable maximum for submarines.

Another potential application is the monitoring of otherwise undetectable disturbances in the ocean, including changes in seismic conditions and the behavior of marine life. This application presents a nonmilitary use for equipment that might otherwise lie unused.

## Appendix A: Equipment Constraints and Resolving Capabilities

A parabolic reflector has constraints dependent on its diameter. Given the diameter  $w$  of our reflector, we can apply Rayleigh's criterion [Pedrotti and Pedrotti 1993, 335], which states that our object must be closer than a fixed distance for the object to be resolved:

$$\theta = \frac{1.22\lambda}{w}. \quad (1)$$

Here,  $\theta$  identifies the minimum angle that can be used to resolve our object, and  $\lambda$  is the wavelength of the sound waves.

Pedrotti and Pedrotti [1993] state that  $\lambda$  is proportional to the speed of sound in water of a certain temperature divided by the frequency of the sound waves. This gives  $\lambda$  as

$$\lambda = \frac{c}{\mu}.$$

Substituting into (1) for  $\lambda$ , we have

$$\theta = \frac{1.22c}{w\mu}.$$

The speed of sound in sea water,  $c$ , is dependent on the temperature of the water. We assume a constant temperature of 25° C. For this temperature,  $c = 1531$  m/s [Lide 1992, 14–31]. The value of  $\mu$  will be determined when we choose the sound wave frequencies to monitor.

We now derive a relation between smallest angle  $\theta$  and the ratio

$$\frac{x = \text{object size}}{r = \text{maximum object distance}}.$$

Assuming that  $\theta$  is a relatively small angle, we have

$$\frac{\theta}{2} \approx \tan\left(\frac{\theta}{2}\right) = \frac{x}{2r}, \quad \frac{x}{r} \approx \frac{1.22c}{w\mu}.$$

**Table 1** lists maximum object distances vs. required reflector diameter to view a  $x = 10$  m-wide object at a frequency view of  $\mu = 40$  kHz. To view an object the width of a submarine at a distance of 20 km, we would need a reflector approximately the length of a submarine, a truly impractical requirement.

## Appendix B: 2-D Example

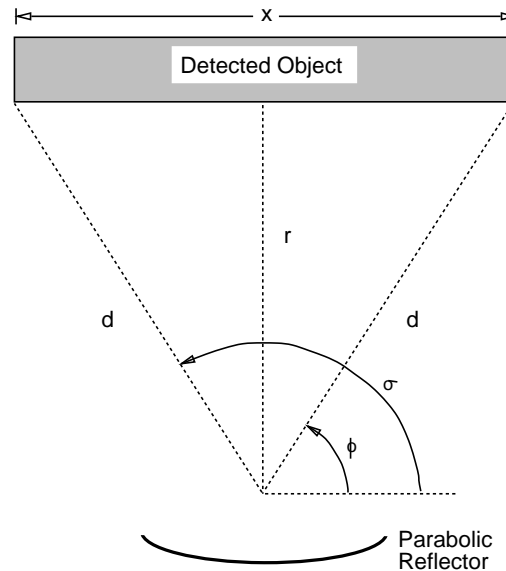
The following example demonstrates what an expected signal response will be for a specific geometrical situation. We consider a specific two-dimensional case with the following conditions (see **Figure 7**):

**Table 1.**

Range vs. required diameter of parabolic reflector.

Distance $r$ (km)	1	2	5	10	20
Diameter $w$ (m)	5	9	23	47	93

- We use a single parabolic reflector.
- The object to detect is a plane line segment, and our sensor lies below the outward normal of the object.
- We measure all angles relative to a line parallel to the line segment. The line segment can be viewed as defining the horizontal. The angle  $\theta$  formed by the horizontal and the normal to the object directed towards the reflector is then  $-90^\circ$ .
- We define several variables for use in our example:
  - The reflector is located directly below the midpoint of the object at a distance  $r = 19.7$  m.
  - The object has a width of  $x = 6.74$  m.
  - The diameter of the reflector is  $w = 5$  m.


**Figure 7.** Relation between object and reflector.

The distance  $d$  from the corner of the object to the center of the reflector is

$$d = \sqrt{\left(\frac{x}{2}\right)^2 + r^2} = 20 \text{ m.}$$

The angle when the center of the reflector is pointed directly at the first corner of the object, measured from a line parallel to the object line segment, is

$$\phi = 90^\circ - \arcsin\left(\frac{x}{2d}\right) = 80^\circ.$$

Similarly, the angle when the center of the reflector is pointing at the last corner of the object is

$$\sigma = 90^\circ + \arcsin\left(\frac{x}{2d}\right) = 100^\circ.$$

To visualize the reflection signal from the object, we must introduce an ambient noise field. Let us assume that we are near the ocean bottom, where seismic disturbances produce a sound field that is more intense when scanning is directed at the sea floor than when scanning is directed upward toward the surface [Stephens 1970, 124–125]. The optical analogy is having the sun at your back while looking into a mirror. We consider a case in which the sound intensity  $I$  of the ambient noise field, with no object in the scan region, depends on the scanning angle  $\lambda$  as follows:

$$I(\lambda) = -2 \sin \lambda + 90.$$

**Figure 8** shows a plot of the function  $I$ .

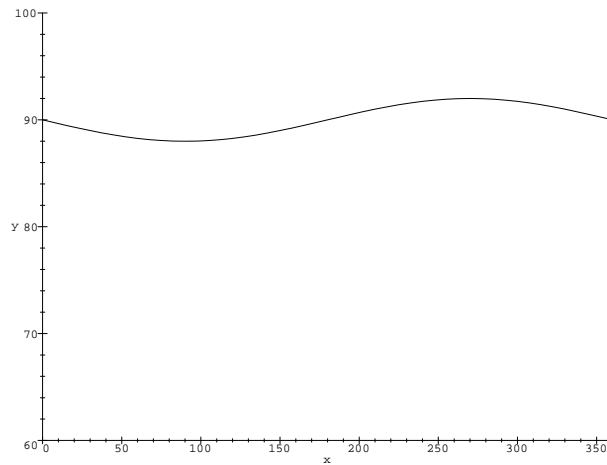


**Figure 8.** Plot of intensity  $I$  vs. scanning angle  $\lambda$  (in degrees).

With an object in the scan region, the reflector begins to pick up reflected noise from the object before being pointed directly at it. **Figure 9** shows the large region  $\Omega$  (between the dotted rays) in which some noise reflected from the object is received. There is a small transition region at each end of the object where the object takes up only part of the view, including a part  $E$  in which the view is mostly of the object. Inside the region  $\Gamma$ , the object is in full view of the reflector and there are no boundary transition effects. Beyond region  $\Omega$ , the signal received is just background noise.

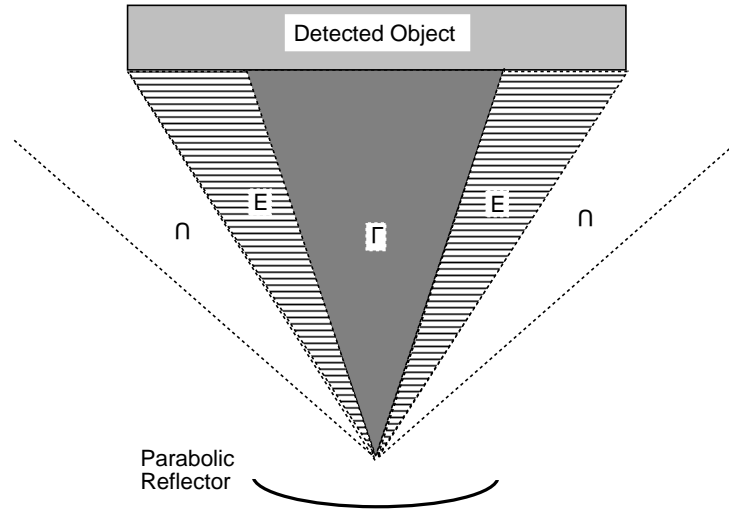


**Figure 9.** Reflected noise is received in region  $\Gamma$  but also in part in region  $E$  and in fact throughout region  $\Omega$  (denoted here by  $\cap$ ), which is bounded by the dotted rays.

The transition region can be described in terms of an angle offset  $\psi$  from the contact angles ( $\sigma$  and  $\phi$ ):

$$\psi = \arcsin\left(\frac{w}{2d}\right),$$

which is shown in **Figure 10**. The outer boundaries of region  $E$  are the angles  $\phi$  and  $\sigma$ ; the boundaries of region  $\Omega$  are angles  $\phi - \psi$  and  $\sigma + \psi$ ; the boundaries of region  $\Gamma$  are the angles  $\phi + \psi$  and  $\sigma - \psi$ . The right-hand transition region corresponds to the angle interval  $(\phi - \psi, \phi + \psi)$ , and the left-hand region to  $(\sigma - \psi, \sigma + \psi)$ , so that each region has angular width  $2\psi$ .

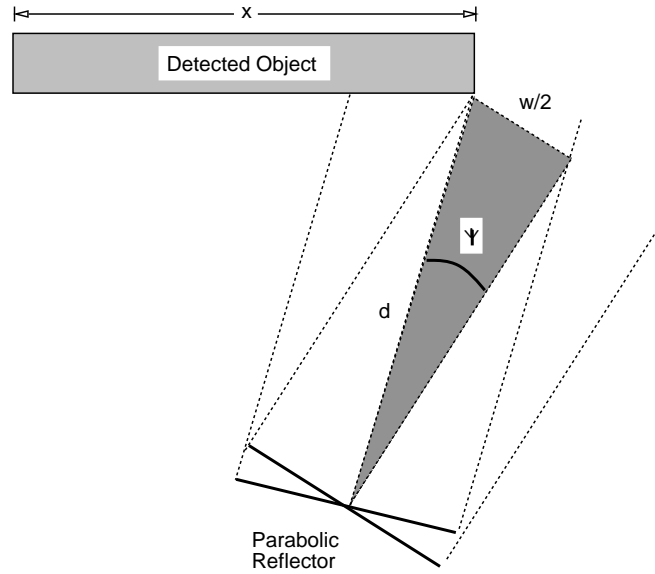


**Figure 10.** Definition of the angle  $\psi$ .

The intensity pattern from inside the region  $\Omega$  depends on the angle between the direction at which the reflector is pointed and the normal from the target object (see **Figure 11**). All sound reaching the reflector must be parallel to the direction at which it is pointed, due to the characteristics of the parabolic shape of the reflector. Following sound from the reflector back to the object reveals from which direction sound is received when reflected.

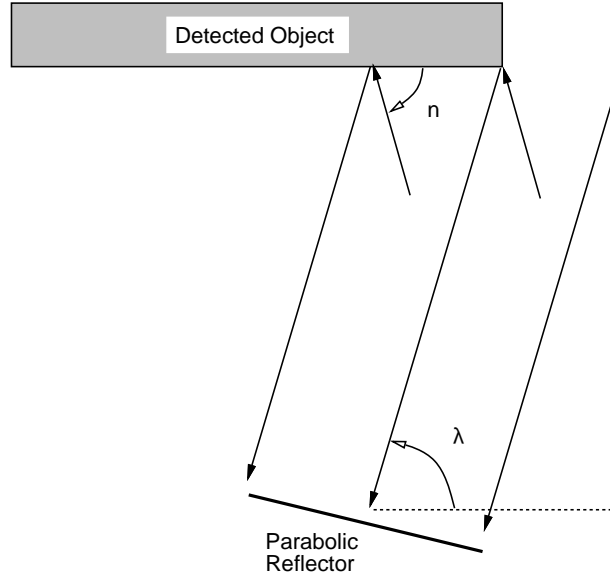


**Figure 11.** The scan angle  $\lambda$  and the view angle  $\eta$ .

The parallel rays from the reflector travel back to the object surface and reflect. The angle of incidence must equal the angle of reflection for a nearly perfect reflective surface. The angle the rays make from the horizontal after reflecting off the surface is

$$\eta(\lambda) = \pi - \lambda - 2\theta.$$

Using this reflected angle equation, we can produce a graph of the reflected intensity when the object takes up the full width of the sensor view, that is, when the object is in region E, where  $\theta$  ranges from  $\phi + \psi$  to  $\sigma - \psi$ . The intensity in this region is given by

$$I(\eta(\lambda)) = 2 \sin\left(\frac{\lambda\pi - 2\pi^2}{180}\right)$$

and is plotted in **Figure 12**.

We approximate the boundary transitions of region  $\Omega$  by fitting a Gaussian that matches the noise intensity of background at region  $\Omega$ 's outer edge and fits the noise reflected intensity at region E's outer edge.

The values of  $I$  in the two boundary regions are

$$I(\eta(\phi + \psi)) e^{\ln\left(\frac{I(\phi - \psi)}{I(\eta(\phi + \psi))}\right)(\lambda - \phi - \psi)^2 / 4\psi^2} = I(\eta(\phi + \psi)) \left[ \frac{I(\phi - \psi)}{I(\eta(\phi + \psi))} \right]^{(\lambda - \phi - \psi)^2 / 4\psi^2},$$

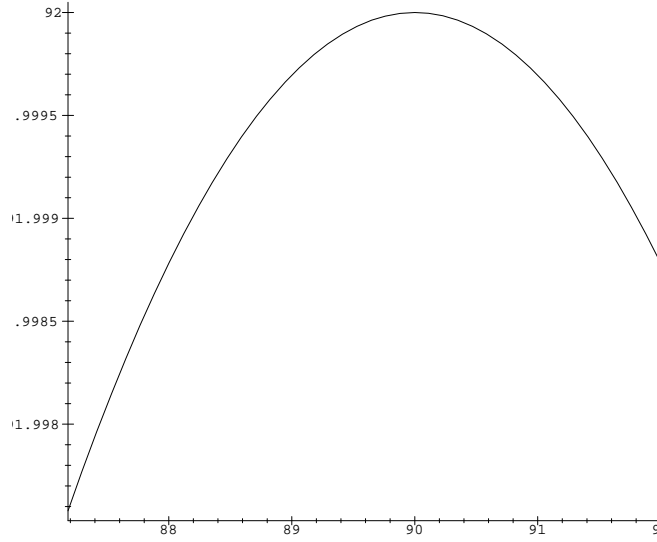


**Figure 12.** Object signal response vs. angle  $\lambda$  (in degrees).

$$I(\eta(\sigma - \psi)) e^{\ln \left( \frac{I(\sigma + \psi)}{I(\eta(\sigma - \psi))} \right) (\lambda - \sigma - \psi)^2 / 4\psi^2} = I(\eta(\sigma - \psi)) \left[ \frac{I(\sigma + \psi)}{I(\eta(\sigma - \psi))} \right]^{(\lambda - \sigma + \psi)^2 / 4\psi^2}.$$

From these expressions, we can build a piecewise function that approximates the noise signal response from the object. Notice that this function is only an approximation, because it is not differentiable at all points. A better approximation can be obtained by fitting derivatives at boundaries as well. **Figure 13** gives a plot of the total intensity response over the entire domain of scan angle  $\lambda$ .

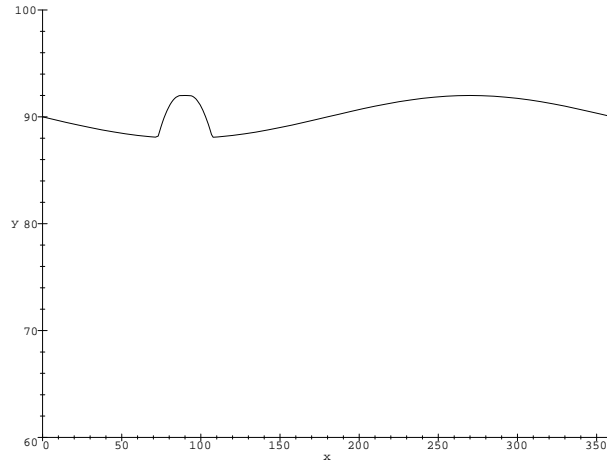


**Figure 13.** Total response vs. angle  $\lambda$  (in degrees).

To isolate the object image, we subtract the background noise field to obtain a difference plot (**Figure 14**). The distinct hump seen there will not always be the case. The intensity response depends on object surface geometry, reflectivity,

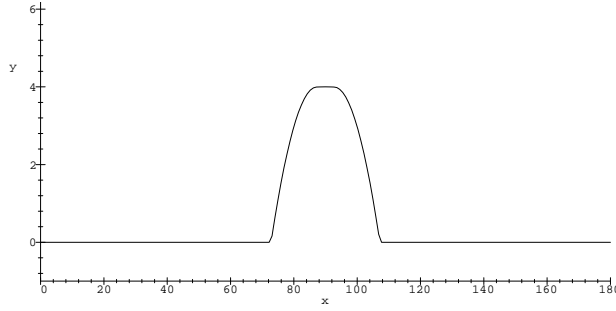


**Figure 14.** Difference plot.

and noise field directional characteristics. Certain parameter values will lead to difference plots that contain hills, valleys, and zero regions inside the overall object intensity response. Note that these complexities do not change the overall process of determining characteristics of the object, as long as a minimum and maximum angles of response can be found.

## Appendix C: Point Location in Two Dimensions

We can determine the location of the object by triangulation from two reflectors, provided the object is not collinear with them (see **Figure 1**). Let  $d_i$  be the distance from reflector  $i$  to the target,  $\theta_i$  the angle formed at reflector  $i$ , and  $\ell$  the distance between the two reflectors.

Applying the law of sines to the triangle formed by the three objects yields

$$\begin{aligned} \frac{d_1}{\sin(\pi - \theta_2)} &= \frac{d_2}{\sin \theta_1} = \frac{\ell}{\sin(\pi - \theta_1 - (\pi - \theta_2))}, \\ \frac{d_1}{\sin \theta_2} &= \frac{d_2}{\sin \theta_1} = \frac{\ell}{\sin(\theta_2 - \theta_1)}. \end{aligned}$$

Solving this for  $d_1$  and  $d_2$  gives

$$d_1 = \frac{\ell \sin \theta_2}{\sin(\theta_2 - \theta_1)}, \quad d_2 = \frac{\ell \sin \theta_1}{\sin(\theta_2 - \theta_1)}. \quad (2)$$

Setting the origin of a coordinate system on reflector 1 and setting the  $x$ -axis to extend along toward reflector 2, the position of the object is then given by the ordered pair  $(x, y) = (d_1 \cos \theta_1, d_1 \sin \theta_1)$ .

## Appendix D: Point Location in Three Dimensions

We assume that two reflectors have located a target and are aimed at it with direction vectors  $\mathbf{v}_1 = \langle a_1, b_1, c_1 \rangle$  and  $\mathbf{v}_2 = \langle a_2, b_2, c_2 \rangle$ . We superimpose a three-dimensional coordinate system on our reflectors with the first reflector located at the origin. For simplicity, we build our coordinate system so that the second reflector lies on the  $x$ -axis a distance  $\ell$  from the first one.



The position of the object is given by the intersection of the two lines with direction vectors  $\mathbf{v}_1$  and  $\mathbf{v}_2$ . The parametric equations for them are

$$\text{line 1 : } \begin{cases} x = s a_1 \\ y = s b_1 \\ z = s c_1 \end{cases}, \quad \text{line 2 : } \begin{cases} x = \ell + t a_2 \\ y = t b_2 \\ z = t c_2 \end{cases} \quad (3)$$

Their intersection is the solution of the system

$$\begin{aligned} s a_1 &= \ell + t a_2 \\ s b_1 &= t b_2 \\ s c_1 &= t c_2 \end{aligned}.$$

With only two unknowns, one equation is redundant. Solving the first two equations for  $s$  gives

$$s = \frac{\ell b_2}{a_1 b_2 - b_1 a_2}. \quad (4)$$

Substituting into (3) gives the location of the object as  $(s a_1, s b_1, s c_1)$ , where  $s$  is given by (4).

## Object Velocity in Two Dimensions

We consider a worked-out example of a plausible trial if reflectors were set up and moved as outlined in this paper. In this scenario, two reflectors are placed on shore 100 m from each other (for this geometry, a third reflector is not needed to resolve the special case when the object and the two reflectors are collinear).

During the first sweep of both reflectors through a full  $180^\circ$ , the reflectors find a peak in the ambient noise plot at angles of  $\theta_1 = 84.3^\circ$  and  $\theta_2 = 91.9^\circ$ . Using (2) from **Appendix C** gives the location of the object:

$$\begin{aligned} x &= \frac{\ell \sin(\theta_2) \cos(\theta_1)}{\sin(\theta_2 - \theta_1)} = \frac{100 \sin(91.9^\circ) \cos(84.3^\circ)}{\sin(91.9^\circ - 84.3^\circ)} = 75.1 \text{ m}, \\ y &= \frac{\ell \sin \theta_1 \sin \theta_2}{\sin(\theta_2 - \theta_1)} = \frac{100 \sin(84.3^\circ) \sin(91.9^\circ)}{\sin(91.9^\circ - 84.3^\circ)} = 752.0 \text{ m}. \end{aligned}$$

Then, 5 sec later, the reflectors find the object at the angles  $\theta_1 = 84.5^\circ$  and  $\theta_2 = 92.4^\circ$ . Using (2) again produces the new location of the object

$$x = 69.7 \text{ m}, \quad y = 723.6 \text{ m}.$$

Subtracting the coordinates gives the direction in which the object has moved:

$$\text{direction} = \langle 69.7 - 75.1, 723.6 - 752.0 \rangle = \langle -5.4, -28.4 \rangle.$$

So, the object is moving predominantly shoreward and slightly toward reflector 1. Its speed is

$$\text{speed} = \frac{\text{distance}}{\text{time}} = \frac{\sqrt{(-5.4)^2 + (-28.4)^2}}{5} = 5.8 \text{ m/s.}$$

Therefore, the object is moving at 5.8 m/s (11 knots) at an angle of 79.2° SSW from the line through both reflectors. When first detected, it is 756 m from the first reflector and 752 m from the second reflector; at the second detection, it is 727 m and 724 m from the reflectors.

## References

- Buckingham, M.J., B.V. Berkhout, and S.A.L. Gregg. 1992. Imaging the ocean with ambient noise. *Nature* 356: 327–329.
- French, A.P. 1971. *Vibrations and Waves*. New York: W.W. Norton.
- Geil, F.G. 1992. Hydrophone techniques for underwater sound pickup. *Journal of the Audio Engineering Society* 40: 711–718.
- Lide, D.R. (ed.). 1992. *CRC Handbook of Chemistry and Physics*. 73rd ed. London: CRC Press.
- Pedrotti, F.L., and L.S. Pedrotti. 1993. *Introduction to Optics*. 2nd ed. Englewood Cliffs, NJ: Prentice Hall.
- Smith, C. 1995. Revisiting solar power's past. *Technology Review* (July 1995). <http://web.mit.edu/afs/athena/org/t/techreview/www/articles/july95/Smith> (11 Feb 1996).
- Stephens, R.W.B. (ed.). 1970. *Underwater Acoustics*. New York: Wiley-Interscience.
- Thornton, S.T., and A. Rex. 1993. *Modern Physics for Scientists and Engineers*. New York: Saunders.
- Toppan, A. 1996. Active USN ships—Submarines. [http://www.wpi.edu/~elmer/navy/current/usn\\_submarines.html](http://www.wpi.edu/~elmer/navy/current/usn_submarines.html) (11 Feb 1996).
- Urick, R.J. 1983. *Principles of Underwater Sound*. 3rd ed. New York: McGraw-Hill.
- Young, H.D. 1992. *University Physics*. 8th ed. New York: Addison-Wesley.